Published in final edited form as:
J Biomech. 2011 March 15; 44(5): 789–793. doi:10.1016/j.jbiomech.2011.01.030.

Invariant hip moment pattern while walking with a robotic hip exoskeleton

Cara L. Lewis, PT, PhD[1] and **Daniel P. Ferris, PhD**[2]

[1]College of Health and Rehabilitation Sciences: Sargent College, Boston University, Boston, MA, USA

[2]School of Kinesiology, University of Michigan, Ann Arbor, MI, USA

Abstract

Robotic lower limb exoskeletons hold significant potential for gait assistance and rehabilitation; however, we have a limited understanding of how people adapt to walking with robotic devices. The purpose of this study was to test the hypothesis that people reduce net muscle moments about their joints when robotic assistance is provided. This reduction in muscle moment results in a total joint moment (muscle plus exoskeleton) that is the same as the moment without the robotic assistance despite potential differences in joint angles. To test this hypothesis, eight healthy subjects trained with the robotic hip exoskeleton while walking on a force-measuring treadmill. The exoskeleton provided hip flexion assistance from approximately 33% to 53% of the gait cycle. We calculated the root mean squared difference (RMSD) between the average of data from the last 15 minutes of the powered condition and the unpowered condition. After completing three 30-minute training sessions, the hip exoskeleton provided 27% of the total peak hip flexion moment during gait. Despite this substantial contribution from the exoskeleton, subjects walked with a total hip moment pattern (muscle plus exoskeleton) that was almost identical and more similar to the unpowered condition than the hip angle pattern (hip moment RMSD 0.027, angle RMSD 0.134, $p<0.001$). The angle and moment RMSD were not different for the knee and ankle joints. These findings support the concept that people adopt walking patterns with similar joint moment patterns despite differences in hip joint angles for a given walking speed.

Keywords

Gait; Inverse dynamics; Joint kinetics; Locomotion; Powered orthosis

1. Introduction

Robotic lower limb exoskeletons hold significant potential for studying human locomotion and for gait assistance and rehabilitation (Ferris et al., 2005; Ferris et al., 2005; Ferris et al., 2007). However, we have a limited understanding of how people adapt to walking with

Corresponding author: Cara Lewis, Human Adaptation Laboratory, College of Health and Rehabilitation Sciences: Sargent College, Boston University, 635 Commonwealth Avenue, Boston, MA, 02215. Phone: (617) 353-7509. lewisc@bu.edu.

Conflict of interest statement – None declared.

robotic devices. Past studies on healthy individuals have found that subjects walking with a robotic ankle-foot exoskeleton reduce their net muscle moment to compensate for the added robotic torque. This reduction in muscle activation results in a consistent total moment (muscle plus exoskeleton) about the joint (Kao et al., 2010a). This finding suggests that joint moments are intrinsically represented in the healthy central nervous system and that the nervous system targets a joint moment profile during unperturbed walking.

While this invariant moment strategy has been demonstrated with robotic assistance at the ankle joint, it is not known if it holds true for more proximal joints. Proximal joints, such as the hip, may behave differently during gait than the ankle joint. It has been suggested that the neural control of lower extremity muscles is affected by a proximodistal gradient (Daley et al., 2007). This premise supposes that proximal joints, such as the hip, are controlled in a feedforward manner while distal joints are more affected by sensory feedback. Thus, the nervous system might adjust muscle activation patterns about the hip joint in response to powered assistance during gait differently compared to how it adjusts muscle activation patterns about the ankle joint in response to powered assistance. Alternatively, if joint moment patterns during gait are intrinsically represented in the central nervous system as a preferred goal (Winter and Eng, 1995), then humans should adjust to robotic hip assistance in a manner similar to robotic ankle assistance (Kao et al., 2010a).

The primary purpose of this study was to test the hypothesis that healthy individuals reduce net muscle moments about their joints when provided with robotic assistance to maintain a consistent total joint moment pattern during walking. We tested this hypothesis by providing appropriately timed mechanical flexion assistance at the hip joint while subjects walked with a pneumatically powered hip exoskeleton. Gaining a deeper understanding of how humans respond to assistance during gait may help direct exoskeleton development for human performance augmentation, assistive technology, and gait rehabilitation (Ferris et al., 2005; Ferris et al., 2005; Ferris et al., 2007). The hip exoskeleton may be particularly beneficial for people with hip pain. If individuals walking with the hip exoskeleton reduce the muscular component of the hip moment, this could reduce hip joint forces. High joint forces are associated with the progression and development of hip osteoarthritis (Mavcic et al., 2004; Recnik et al., 2007).

2. Methods

2.1 Subjects

Eight healthy, neurologically intact subjects (5 males, 3 females; age 30.8±7.4 years; mass 80.1±15.0 kg; height 1.8±0.1 m) gave written informed consent and participated in this study. The University of Michigan Medical School Institutional Review Board approved this protocol, and the study conformed to the standards sets by the Declaration of Helsinki.

2.2 Powered hip exoskeleton

We created a pneumatically powered hip exoskeleton to assist hip flexion during gait (Ferris and Lewis, 2009). The powered hip exoskeleton consisted of a prefabricated hip brace (OPTEC, Inc, Lawrenceville, GA, USA) modified to include a pneumatic actuator (Figure 1). Unlike other exoskeletons we have created which used artificial pneumatic muscles (Gordon and Ferris, 2007; Kao and Ferris, 2009; Kao et al., 2010a; Kinnaird and Ferris, 2009), the hip exoskeleton had two pneumatic cylinders providing external joint torques. Steel brackets were added to attach the cylinders to the pelvic portion and each thigh portion of the exoskeleton. A low profile tension / compression load cell (OMEGA Engineering, Inc, Stamford, CT, USA) placed in series with the pneumatic cylinders quantified assistance

provided by the robotic exoskeleton. We also added a polypropylene lumbosacral support to provide additional stability to the exoskeleton.

2.3 Control Method

We used a footswitch based control signal to regulate air pressure to the pneumatic cylinder during a predetermined portion of the gait cycle (Figure 2). Heel strike, as determined by the footswitch, was used to create a moving window average stride time over the previous 10 strides for each leg. Custom software and a real-time control board (dSPACE, Inc, Wixom, MI, USA) regulated the air pressure in the pneumatic cylinders to coincide with the normal onset of the hip flexion muscle moment. In pilot studies, we determined that sending a 10 V control signal to the pressure regulators from approximately 30% through 50% of the gait cycle produced an exoskeleton torque curve that closely matched the hip flexion muscle moment curve (Figure 4). The exoskeleton torque curve is slightly delayed due to the mechanics of the pneumatic system (Gordon et al., 2006). The control algorithm was adaptive in that the average stride time, calculated over the previous 10 strides, was updated every step to account for changes in a subject's cadence. This allowed the robotic device to remain synchronized with the gait cycle, which was critical for maintaining consistent and appropriately timed mechanical assistance (Aoyagi et al., 2007).

2.4 Experimental protocol

Subjects completed three testing sessions at least three days apart each. During each session, subjects walked while wearing the exoskeleton unpowered ("passive") for 10 minutes and with the exoskeleton providing hip flexion assistance for 30 minutes ("powered"). Subjects walked at a speed of 1.25 m/s on a custom built split-belt force-measuring treadmill (Collins et al., 2009) (1200 Hz). We used a motion capture system (Motion Analysis Corp., Santa Rosa, CA, USA) (120 Hz) and retroreflective markers to record the kinematics of the ankle, knee and hip joints. The marker set was a modification of a previously published marker set (McLean et al., 2008). Briefly, we placed markers on the posterior heel, 5^{th} metatarsal head and lateral malleolus, a marker cluster on the shank, three markers on the anterior thigh, and four markers on the pelvic component of the exoskeleton (one over each posterior superior iliac spine and one above each anterior superior iliac spine). We also collected a static trial with the subject standing in a neutral position. For the static trial, we had additional markers on the medial malleoli, medial and lateral femoral condyles, greater trochanters and anterior superior iliac spines. We used commercial software (Visual3D, C-Motion, Inc, Germantown, MD, USA) to calculate joint angles based on a 3-dimensional model (McLean et al., 2008) and kinetics by inverse dynamics analysis. We also calculated the torque due to the exoskeleton using the cylinder position (120 Hz) and cylinder force data from the load cell (1200 Hz). To calculate exoskeleton torque, we placed reflective tape around the connections of the pneumatic cylinder to the exoskeleton and a reflective marker over the exoskeleton joint. We calculated the cross product of the vector from the exoskeleton joint to the top of the actuator and the cylinder force vector along the line of the actuator. In this paper, we restricted our analyses to the sagittal plane.

2.5 Data acquisition and analysis

We collected kinematic, kinetic and actuator force data for the first 10 seconds of every minute during each condition. We averaged the data for the 10-minute passive condition and for the last 15 minutes of the powered condition to obtain mean curves over the gait cycle for each variable. Gait cycle was defined as left heel strike, as determined by the vertical ground reaction force, to ipsilateral heel strike. The variables calculated were the ankle, knee and hip angles, moments and powers, and exoskeleton torque. We also calculated the root mean squared difference (RMSD) between the mean gait cycle curves for the passive condition and the mean gait cycle curve for data from the last 15 minutes of the powered

condition for each subject. The RMSD for each variable was normalized from 0 to 1 for the range of that variable to allow for comparison between variables of different magnitudes. Additionally we calculated the normalized RMSD for the mean curve for each minute of powered walking to evaluate steady-state behavior.

2.6 Statistical tests

We used paired t-tests to compare the angle RMSD to the moment RMSD for the ankle, knee and hip joints. This comparison allowed us to determine if the joint moment curves were more similar across conditions than were the joint angle curves. To confirm that our subjects were at steady-state during the last 15 minutes of the third day of training with the exoskeleton, we also calculated the slope of the minute RMSD plotted over time for the last 15 minutes of the powered condition for each variable (Figure 3). We used a one-sample t-test to determine if the slope was different from zero. A slope that is different from zero would indicate that the variable is still changing in the last 15 minutes of the third day and had not reached steady-state.

We used paired t-tests to compare the positive and negative work performed by the exoskeleton and by the total hip complex (biological hip plus exoskeleton) between the passive condition and the last 15 minutes of the powered condition. All statistical analyses were conducted in PASW 18 (SPSS: An IBM Company, Chicago, IL, US) and Bonferroni correction was used to account for multiple t-tests. A corrected *p*-value less than 0.05 was considered significant. This adjustment method is equivalent to dividing the alpha-level by the number of comparisons.

3. Results

Subjects walking with the powered hip exoskeleton had reached a steady-state by the end of the 3rd day of training. This is indicated by the zero slope of the RMSDs for the last 15 minutes of the powered condition for the ankle, knee and hip angle, moment and power.

The pneumatically powered hip exoskeleton peak moment was 27.1% ± 10.6% (mean ± standard deviation) of the peak hip flexion moment during gait. The peak hip exoskeleton moment occurred slightly before the peak hip flexion moment (51% ± 1.6% and 53% ± 1.3% of the gait cycle respectively). Despite this substantial torque generation, the total hip moment curves of the passive and the last 15 minutes of the powered condition were almost identical (Figure 4). The hip angle curve of the powered condition demonstrated differences compared to the hip angle curve of the passive condition (Figure 3). The difference between the angle curves (Hip Angle RMSD) was significantly greater than the difference between the hip moment curves (Hip Moment RMSD) ($p<0.001$) (Table 1). For the knee and ankle joints, however, the Angle RMSD and the Moment RMSD were not different from each other ($p>0.08$).

In addition to the similarity in the hip moment curves between conditions, the positive work done by the total hip complex (biological hip plus exoskeleton) was not different between conditions ($p = 0.272$) (Table 2). This occurred despite the exoskeleton providing 12.0% ± 5.3% of the total positive hip work. The negative work done by the total hip complex was lower ($p = 0.002$) in the powered condition than in the passive condition with the hip exoskeleton contributing 18.8% ± 15.7 of the total negative work during the powered condition.

4. Discussion

The findings of this study support the hypothesis that humans alter the net muscle moment at the hip joint during walking with powered hip assistance so that the total joint moment is the same with and without additional hip exoskeleton torque. Despite the hip exoskeleton providing approximately 23 Nm of hip flexion torque, the total hip joint moment curve during the last 15 minutes of the powered condition was very similar to the hip joint moment curve during the passive condition. The hip angle curves, however, were not similar. As the hip exoskeleton became active during the gait cycle (~32% of the gait cycle), the motion into hip extension was restricted, reducing the total hip extension excursion.

Reducing the muscular component of the hip moment may be beneficial for people with hip pain. As the majority of the hip joint force during gait is due to muscular contraction (Krebs et al., 1998; Lewis et al., 2010), this reduction in the hip moment should also lessen the joint force, and thereby may slow the development or progression of hip osteoarthritis (Mavcic et al., 2004; Recnik et al., 2007). Limiting the maximum hip extension angle may be additionally beneficial for people with an anterior acetabular labral tear. A high percentage of these anterior labral tears, up to 74.1% (Santori and Villar, 2000), occur in the absence of major trauma. These non-traumatic tears are thought to be caused by repetitive microtrauma (Mason, 2001; McCarthy et al., 2001) due to high forces on the anterior hip structures. Using musculoskeletal modeling, Lewis and colleagues have demonstrated that the anterior hip joint forces are greatest in hip extension (Lewis et al., 2010), especially when hip flexors are activated (Lewis et al., 2009). Therefore, a device which both reduces hip extension and provides hip flexion torque may be particularly beneficial for a person with an anterior acetabular labral tear. While the current hip exoskeleton is not easily portable, there are a number of similar devices in development, such as the Honda's Walk Assist Device with Stride Management System (http://corporate.honda.com/innovation/walk-assist) that could serve this function in a fully portable manner.

The powered hip exoskeleton may also be useful for patients who are unable to independently produce the normal hip flexion moment during gait, such as patients with myopathies affecting the proximal muscles. As the magnitude of the exoskeleton torque can be controlled in real-time, the exoskeleton could be used as a progressive training device providing just enough assistance to compensate for the weakened muscles. This would allow the patient to walk with the normal moment pattern despite muscular weakness. However, it is not yet clear how elderly individuals or individuals with pathology would adjust net muscle moments while walking with the powered assistance.

Combined with other previously published results, the current findings indicate that the human nervous system seems to have a preferred pattern of joint moments during walking. In our past studies, we found that humans adjusting to a robotic ankle exoskeleton maintained a consistent total ankle joint moment for both powered assistance and unpowered assistance (Kao et al., 2010a). This consistent joint moment pattern even occurred when the ankle exoskeleton was unexpectedly turned off during walking (Kao et al., 2010b). In the unexpected perturbation case, reflexes quickly provided enhanced muscle recruitment and a consistent total ankle moment pattern (Kao et al., 2010b). In a related manner, another previous study found that swing leg dynamics followed a kinetic rule of intra-limb coordination in humans during walking (Shemmell et al., 2007). Joint moments at the ankle, knee, and hip were linearly scaled with each other so that knowing a single joint torque was enough to predict the other two torque patterns. All of these findings are congruent and suggest that joint kinetics are inherently represented in nervous system planning during human walking. Importantly, all of the previously published studies and this paper also provide evidence that joint kinematic patterns are relatively less important to

nervous system planning. Future studies should examine human walking with more complex lower limb exoskeletons to determine if the principle of torque pattern invariance holds for other exoskeletons. This is particularly important if the results are to be used in the design of new exoskeleton devices and estimating their mechanical power requirements.

Acknowledgments

The authors would like to thank Anne Manier for help with fabricating the exoskeleton. We also thank the members of the Human Neuromechanics Laboratory for assistance in collecting and processing data. Supported by NIH F32 HD055010 (CLL) and R21 NS062119 (DPF).

References

Aoyagi D, Ichinose WE, Harkema SJ, Reinkensmeyer DJ, Bobrow JE. A robot and control algorithm that can synchronously assist in naturalistic motion during body-weight-supported gait training following neurologic injury. IEEE Transactions on Neural Systems and Rehabilitation Engineering. 2007; 3:387–400. [PubMed: 17894271]

Collins SH, Adamczyk PG, Ferris DP, Kuo AD. A simple method for calibrating force plates and force treadmills using an instrumented pole. Gait & Posture. 2009; 1:59–64. [PubMed: 18755590]

Daley MA, Felix G, Biewener AA. Running stability is enhanced by a proximo-distal gradient in joint neuromechanical control. The Journal of Experimental Biology. 2007; (Pt 3):383–394. [PubMed: 17234607]

Ferris DP, Czerniecki JM, Hannaford B. An ankle-foot orthosis powered by artificial pneumatic muscles. Journal of Applied Biomechanics. 2005; 2:189–197. [PubMed: 16082019]

Ferris, DP.; Lewis, CL. Robotic lower limb exoskeletons using proportional myoelectric control; Conference Proceedings: IEEE Engineering in Medicine and Biology Society; 2009. p. 2119-2124.

Ferris DP, Sawicki GS, Daley MA. A Physiologist's Perspective on Robotic Exoskeletons for Human Locomotion. International Journal of Humanoid Robotics. 2007; 3:507–528. [PubMed: 18185840]

Ferris DP, Sawicki GS, Domingo A. Powered lower limb orthoses for gait rehabilitation. Topics in Spinal Cord Injury Rehabilitation. 2005; 2:34–49. [PubMed: 16568153]

Gordon KE, Ferris DP. Learning to walk with a robotic ankle exoskeleton. Journal of Biomechanics. 2007; 12:2636–2644. [PubMed: 17275829]

Gordon KE, Sawicki GS, Ferris DP. Mechanical performance of artificial pneumatic muscles to power an ankle-foot orthosis. Journal of Biomechanics. 2006; 10:1832–1841. [PubMed: 16023126]

Kao PC, Ferris DP. Motor adaptation during dorsiflexion-assisted walking with a powered orthosis. Gait & Posture. 2009; 2:230–236. [PubMed: 18838269]

Kao PC, Lewis CL, Ferris DP. Invariant ankle moment patterns when walking with and without a robotic ankle exoskeleton. Journal of Biomechanics. 2010a; 2:203–209.

Kao PC, Lewis CL, Ferris DP. Joint kinetic response during unexpectedly reduced plantar flexor torque provided by a robotic ankle exoskeleton during walking. Journal of Biomechanics. 2010b; 7:1401–1407.

Kinnaird CR, Ferris DP. Medial gastrocnemius myoelectric control of a robotic ankle exoskeleton. IEEE Transactions on Neural Systems and Rehabilitation Engineering. 2009; 1:31–37. [PubMed: 19211321]

Krebs DE, Robbins CE, Lavine L, Mann RW. Hip biomechanics during gait. Journal of Orthopaedic and Sports Physical Therapy. 1998; 1:51–59. [PubMed: 9653690]

Lewis CL, Sahrmann SA, Moran DW. Effect of hip angle on anterior hip joint force during gait. Gait & Posture. 2010; 4:603–607. [PubMed: 20934338]

Lewis CL, Sahrmann SA, Moran DW. Effect of position and alteration in synergist muscle force contribution on hip forces when performing hip strengthening exercises. Clinical Biomechanics (Bristol, Avon). 2009; 1:35–42.

Mason JB. Acetabular labral tears in the athlete. Clinics in Sports Medicine. 2001; 4:779–790. [PubMed: 11675886]

Mavcic B, Slivnik T, Antolic V, Iglic A, Kralj-Iglic V. High contact hip stress is related to the development of hip pathology with increasing age. Clinical Biomechanics (Bristol, Avon). 2004; 9:939–943.

McCarthy JC, Noble PC, Schuck MR, Wright J, Lee J. The Otto E. Aufranc Award: The role of labral lesions to development of early degenerative hip disease. Clinical Orthopaedics and Related Research. 2001; 393:25–37. [PubMed: 11764355]

McLean SG, Huang X, van den Bogert AJ. Investigating isolated neuromuscular control contributions to non-contact anterior cruciate ligament injury risk via computer simulation methods. Clinical Biomechanics (Bristol, Avon). 2008; 7:926–936.

Recnik G, Kralj-Iglic V, Iglic A, Antolic V, Kramberger S, Vengust R. Higher peak contact hip stress predetermines the side of hip involved in idiopathic osteoarthritis. Clinical Biomechanics (Bristol, Avon). 2007; 10:1119–1124.

Santori N, Villar RN. Acetabular labral tears: result of arthroscopic partial limbectomy. Arthroscopy. 2000; 1:11–15. [PubMed: 10627339]

Shemmell J, Johansson J, Portra V, Gottlieb GL, Thomas JS, Corcos DM. Control of interjoint coordination during the swing phase of normal gait at different speeds. Journal of Neuroengineering and Rehabilitation. 2007; 10

Winter DA, Eng P. Kinetics: our window into the goals and strategies of the central nervous system. Behavioural Brain Research. 1995; 2:111–120. [PubMed: 7779286]

Figure 1.
The bilateral pneumatically powered hip exoskeleton: front (left) and side (right) views. The adjustable exoskeleton consists of a bivalve thigh cuff and a pelvic band, with an added polypropylene lumbosacral support. The thigh and pelvis sections are connected with a joint which allows both flexion and extension, and abduction and adduction. Steel brackets were added for the attachment of the pneumatic cylinder.

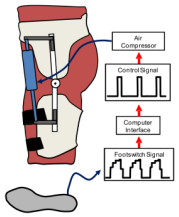

Figure 2.
The robotic hip exoskeleton uses the signal from the footswitch to detect heel strike. Based on the average stride time, a 10V control signal is sent to the pressure regulators during the specified portion of the stride cycle. As air pressure increases, the pneumatic cylinder shortens to assist with hip flexion.

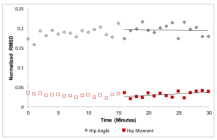

Figure 3.
Normalized root mean squared difference (RMSD) was calculated using the mean data from each minute of the powered condition compared to the mean of the passive condition. We fit the last 15 minutes of RMSD data point (solid symbols) with a line. We compared the slope of the line to zero to confirm that subjects had reached a steady state by the last 15 minutes of powered walking on the third day. Data are from a representative subject.

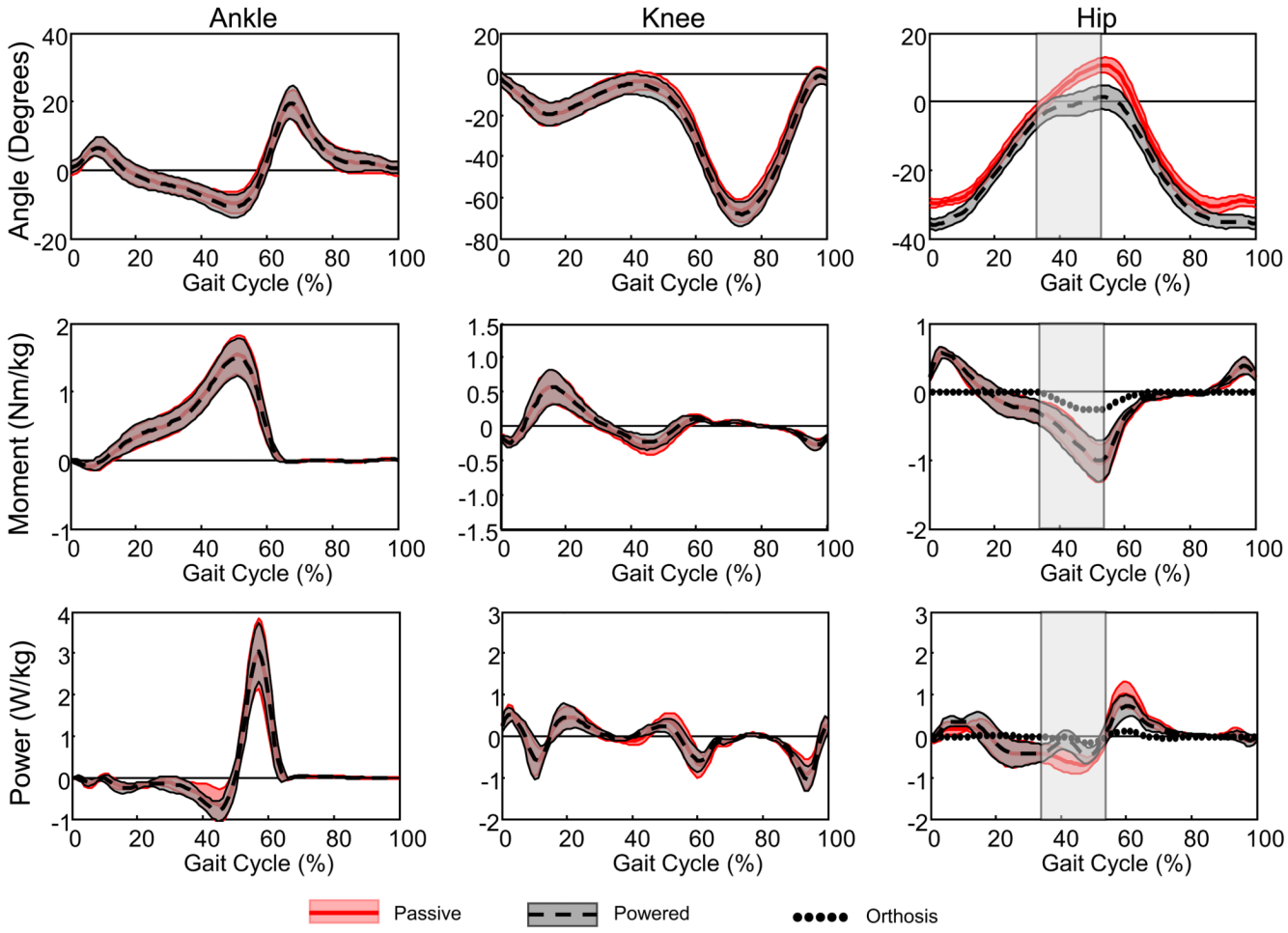

Figure 4.

Ankle, knee and hip joint kinematic and kinetic data. Data represents the mean for all eight subjects walking during the passive condition (thick red line represents the mean and thin red lines are ± one standard deviation) and during the last 15 minutes of the powered condition (thick black dashed line and thin black lines are ± one standard deviation). Dotted lines represent the contribution from the hip exoskeleton. Ankle plantar flexion, knee extension and hip extension are positive. The hip orthosis provided hip flexion assistance from approximately 33% to 53% of the gait cycle (gray vertical shaded region).

Table 1

The normalized root mean squared distance (RMSD) between the passive condition and the last 15 minutes of the powered condition for the hip angle curve is significantly greater than the RMSD for hip moment curve (*). The RMSD for the angle and moment curves at the knee and ankle are not different.

	Normalized RMSD		
Joint	**Angle**	**Moment**	**Adjusted p-value**
Hip	0.134 ± 0.050	0.027 ± 0.008	<0.001*
Knee	0.034 ± 0.020	0.050 ± 0.031	0.181
Ankle	0.039 ± 0.021	0.021 ± 0.008	0.084

Table 2

Positive and negative mechanical work at the hip joint performed by the total hip (biological muscle and exoskeleton) and by the exoskeleton alone during the passive condition and during the last 15 minutes of the powered condition. The total hip negative work is significantly lower in the powered condition compared to the passive condition (*).

	Passive	Powered	Adjusted p-value
Total hip			
Positive work (W/kg)	0.18 ± 0.04	0.16 ± 0.03	0.272
Negative work (W/kg)	0.20 ± 0.10	0.15 ± 0.09	0.002*
Exoskeleton			
Positive work (W/kg)	< 0.01	0.02 ± 0.01	N/A
Negative work (W/kg)	< 0.01	0.02 ± 0.01	N/A